

# BLDC MOTOR SIMULATION USING MAGNETO

## ABSTRACT

The magnetostatic characteristics of an 8-pole, 12 slot brushless DC motor were simulated on a model 70 IBM PS/2 with math-coprocessor chip. Version 2.0 of the MAGNETO Magnetic Field Solver two-dimensional, boundary-element method program from Integrated Engineering Software Inc., was used. Non-linear magnetic material properties were used. Results included contour and arrow maps of fields, graphs of normal and tangential fields in the gap, and calculations of torque vs rotor angle, radial forces vs miscentering of rotor to stator, and inductance. The calculated results were in good agreement with experimental results.

### Integrated Engineering Software - Website Links

[Home](#)[Products](#)[Support](#)[Technical Papers](#)

*"Page Down" or use scroll bars to read the article*

## BLDC MOTOR SIMULATION USING MAGNETO©

D.W. Chapman

IBM Corporation, General Products Division  
5600 Cottle Road, San Jose, CA 95193, U.S.A.

**Abstract** – The magnetostatic characteristics of an 8-pole, 12 slot brushless DC motor were simulated on a model 70 IBM PS/2 with math-coprocessor chip. Version 2.0 of the MAGNETO Magnetic Field Solver two-dimensional, boundary-element method program from Integrated Engineering Software Inc., was used. Non-linear magnetic material properties were used. Results included contour and arrow maps of fields, graphs of normal and tangential fields in the gap, and calculations of torque vs rotor angle, radial forces vs miscentering of rotor to stator, and inductance. The calculated results were in good agreement with experimental results.

### INTRODUCTION

The MAGNETO software was chosen because of its “user friendly” character [1]. With no prior magnetic simulation, personal computer, or motor experience, the author was able to produce useful simulation results within a few weeks. We were also interested to see how well the results from such a two-dimensional program would agree with experimental results. The motor we simulated has an outside diameter which is 15% to 20% greater than its axial length. The motor is delta wound.

### PROCEDURE AND RESULTS

The instructions in the MAGNETO User and Technical Manual were easily followed [2]. The geometry shown in Figure 2 and the materials magnetic properties shown in Figure 3, 4, and 5 were entered into the PS/2; initially, a lesser number of elements and points, etc., than the number listed in Figure 2 were used. A small number of torque values on a tentative torque vs rotor-angle curve were calculated to find the rotor position near the peak torque occurrence. Then the torque at that and one or two other positions was calculated by using an increasing number of elements, points, and segments until there was no significant change in the torque value. Fortunately, the 500 maximum number of elements allowed by the program was sufficient. Essentially all 500 were also required, which resulted in a approximately 8-hour run-time to calculate each torque value. The batch mode of MAGNETO operation was therefore used to calculate batches of points in overnight and over-the-weekend runs to complete the torque vs rotor angle curve shown in Figure 10. Both the peak torque and the average torque constant over the 15-degree computation period agreed with experimental results within a few per cent. A measured torque vs rotor angle curve for one of the motors is show in Figure 11.

Knowing the required number of elements, the field maps and graphs shown in Figures 6 through 9 were routinely generated following the User Manual instructions. It was also possible to radially displace the rotor with respect to the center of the stator and calculate the radial force due to the miscentering, which yielded a graph like that shown in Figure 12.

Finally, the inductance was calculated from the 12-row by 12-column inductance matrix obtained from MAGNETO. Because there was not room for 12 columns in the display and printer, the 12 columns are folded over into three printed rows of four columns each for each “matrix row,” as illustrated in Table 1. The circuit diagram of the windings and the equations used to calculate the inductance are show below [3]. The self and mutual inductance terms were calculated by putting the inductance matrix into a DOS file on the PS/2 hard disk and transmitting it to a host computer where APL was used. The calculated effective inductance is about 30% larger than the inductance measured on the first few motors made. The reason for the difference has not been determined.

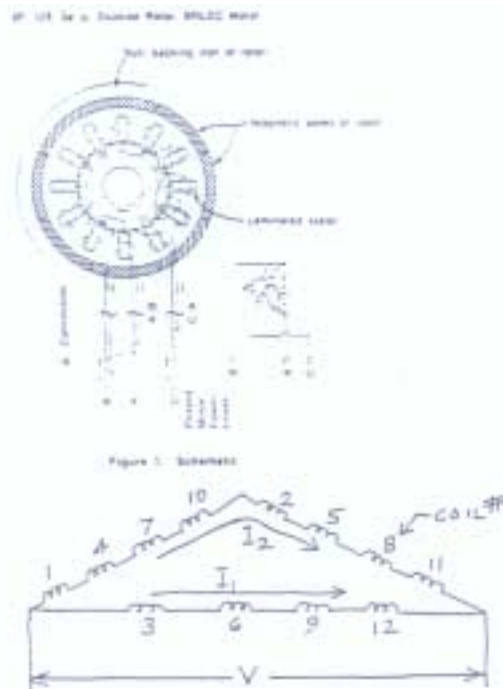


Figure 1. Schematic

$$V = L_1 \frac{di_1}{dt} + M \frac{di_2}{dt}$$

$$= L_2 \frac{di_2}{dt} + M \frac{di_1}{dt}$$

where  $L_1 = \sum_{i=j=2,3,9,12} \ell_{ij}$

and  $L_2 = \sum_{i=j=1,2,4,7,8,10,11} \ell_{ij}$

and  $M = \sum_{i=2,3,9,12} \ell_{ij} = \sum_{i=1,2,4,7,8,10,11} \ell_{ij}$

and  $\ell_{ij}$  = row  $i$ , column  $j$ , term of the inductance matrix.

Finally,  $L_{\text{EFFECTIVE}} = \frac{L_1 L_2 - M^2}{L_1 + L_2 - 2M}$  = effective inductance



Figure 2. Geometry

500 Elements  
219 Segments  
242 Points  
36 Regions

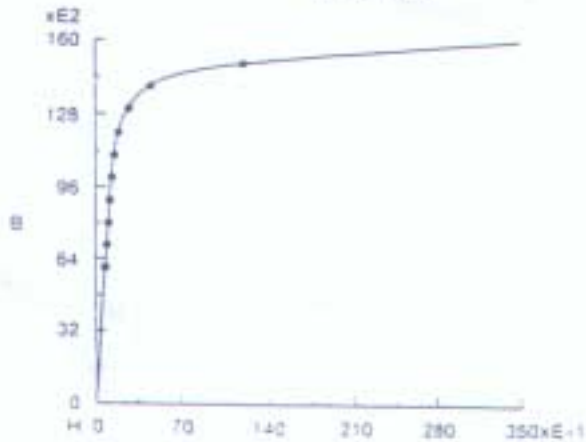


Figure 1. Laminations

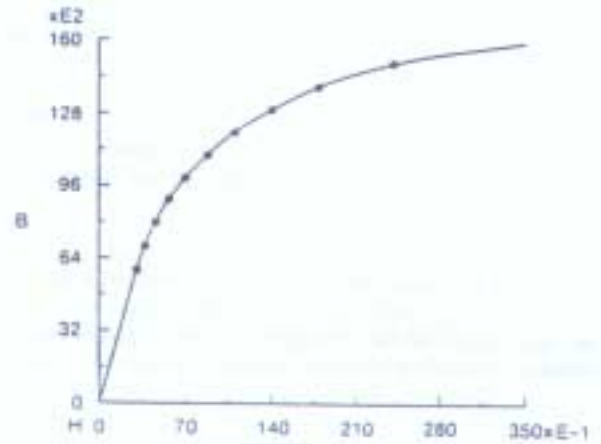


Figure 4. Backing Iron

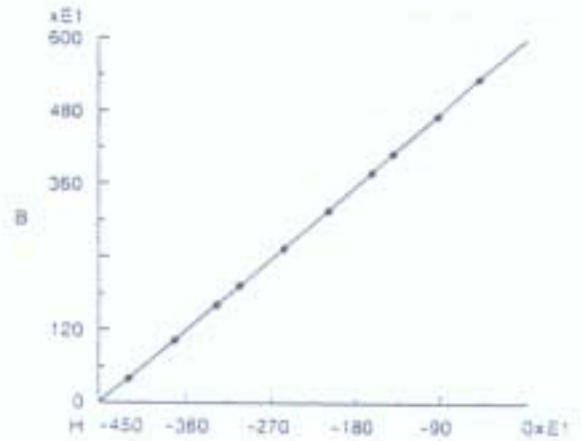


Figure 5. Magnets

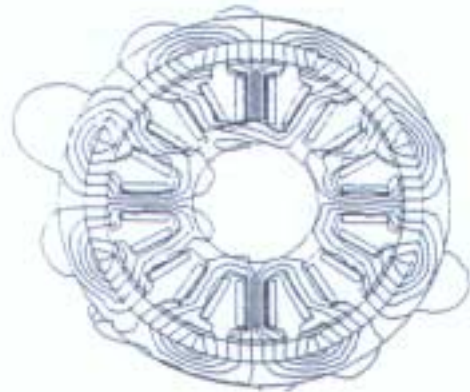


Figure 6. Field Contour Map

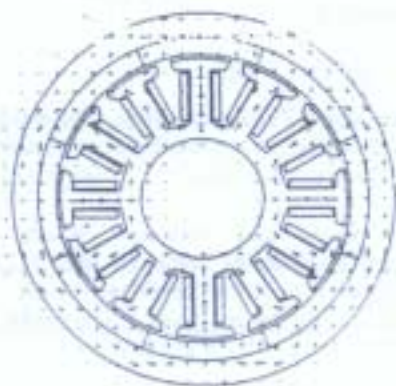


Figure 7. Field Arrows

8 Pole, 12 Slot  
500 Elements, 219 Segments, 242 Points, 36 Regions

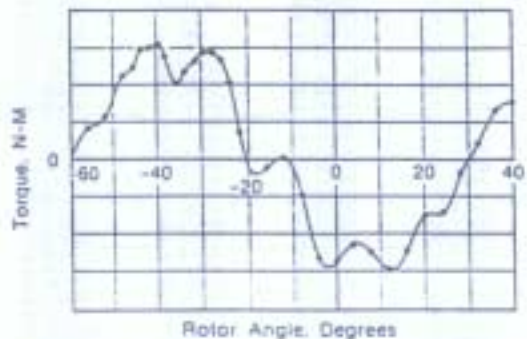


Figure 10. Torque vs Rotor Angle, Calculated by Magneto

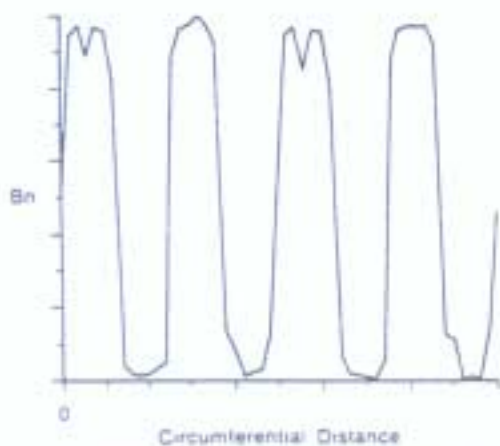


Figure 8. Airgap-B $\perp$  to Magnets



Figure 11. Measured Torque vs Angle

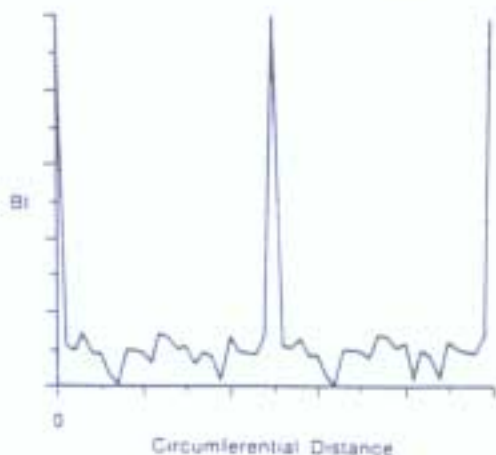


Figure 9. Airgap-B Tangent to Magnets

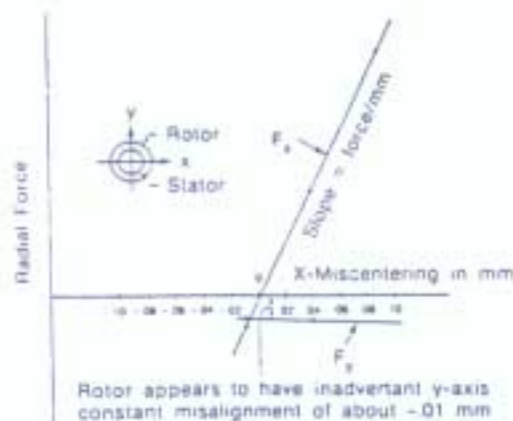


Figure 12. Radial Forces vs Miscentering of Rotor to Stator Calculated with Magneto

Table 1. Inductance Matrix:

row	column 1	column 2	column 3	column 4
1	9.1221E-05	2.6788E-05	4.8800E-06	4.0014E-06
2	2.0286E-05	8.0947E-05	2.0705E-05	5.0775E-05
3	4.3222E-06	4.0786E-06	4.3314E-06	4.3589E-06
4	4.8800E-06	2.0705E-05	8.4396E-05	2.0996E-05
5	4.0014E-06	5.0775E-05	4.0276E-06	4.0254E-06
6	4.3589E-06	4.3314E-06	4.4512E-06	2.8427E-06
7	4.7866E-06	4.6096E-06	4.6736E-06	2.2563E-05
8	4.6096E-06	1.8992E-05	5.2547E-06	4.7466E-06
9	4.6736E-06	4.6096E-06	4.5674E-06	2.8648E-06
10	2.2563E-05	2.7966E-06	3.6774E-06	4.3533E-06
11	4.7466E-06	4.7466E-06	2.0972E-05	4.4129E-06
12	2.8648E-06	4.2126E-06	4.9657E-06	2.4554E-06
13	4.4253E-06	4.2244E-06	4.0196E-06	4.8728E-06
14	5.2547E-06	2.0972E-05	8.9147E-05	2.2201E-05
15	4.7188E-06	4.9206E-06	4.7246E-06	2.8874E-06
16	4.2678E-06	4.2506E-06	4.0547E-06	4.2262E-06
17	4.1486E-06	4.4136E-06	2.2201E-05	8.6549E-05
18	1.8927E-05	5.0115E-06	4.7004E-06	2.7529E-06
19	4.1057E-06	4.1525E-06	2.7577E-06	4.0917E-06
20	4.2182E-06	2.8151E-06	4.1186E-06	1.8217E-05
21	5.2682E-05	2.1927E-05	1.8227E-06	2.6229E-06
22	4.8688E-06	4.1096E-06	4.2131E-06	4.5292E-06
23	4.6827E-06	4.2118E-06	4.8206E-06	5.0115E-06
24	2.1927E-05	5.0115E-06	2.4248E-05	4.2695E-06
25	1.1730E-06	4.6875E-06	4.2675E-06	4.4512E-06
26	1.8674E-06	4.6827E-06	4.7214E-06	4.7004E-06
27	4.6527E-06	2.4248E-05	9.5845E-05	1.8849E-05
28	2.6574E-05	4.5675E-06	2.8708E-06	2.8427E-06
29	2.8648E-06	2.4554E-06	2.8874E-06	2.7529E-06
30	2.8629E-06	4.2695E-06	1.8849E-05	4.0415E-05

## ACKNOWLEDGMENTS

Two IBM San Jose coworkers assisted in this work: Wade Cole provided initial help on the use of MAGNETO, and David Heim provided consultation on the inductance calculations.

## REFERENCES

1. N.J. Haakonstad, PC-Based BEM Software, Proceedings of 1990 Symposium on Incremental Motion Control Systems & Devices, San Jose, CA, June 12-14, 1990.
2. MAGNETO Users and Technical Manual, Version 2.0, Integrated Engineering Software, Inc., 3135 S. State Street, Suite 300, Ann Arbor, Michigan 48108.
3. E.R. Peck, Electricity and Magnetism, McGraw-Hill Book Co., Inc., N.Y., p 261 (1953).